Comparative study of differently treated animal bones for Co^{2+} removal

S. Dimović [a,*], I. Smičiklas [a], I. Plećaš [a], D. Antonović [b], M. Mitrić [a]

[a] Institute of Nuclear Sciences "Vinča", P.O. Box 522, 11000 Belgrade, Serbia
[b] Faculty of Technology and Metallurgy, Karnegijeva 4, 11000 Belgrade, Serbia

ARTICLE INFO

ABSTRACT

The objective of the present study was the evaluation of differently treated bovine bones for Co^{2+} removal from aqueous media. Powdered bones (B), as well as samples prepared by H$_2$O$_2$ oxidation (BH$_2$O$_2$) and annealing at 400–1000 °C (B400–B1000), were tested as sorbent materials. A combination of XRD, FTIR spectroscopies, DTA/TGA analyses, specific surface area (S_p) and point of zero charge (pH$_{PZC}$) measurements was utilized for physicochemical characterization of sorbents. Sorption of Co^{2+} was studied in batch conditions as a function of pH, contact time and Co^{2+} concentration. Initial pH values in the range 4–8 were found optimal for sorption experiments. Equilibrium time of 24 h was required in all investigated systems. The maximum sorption capacities differ significantly from 0.078 to 0.495 mmol/g, whereas the affinity towards Co^{2+} decreased in the order: B400 > BH$_2$O$_2$ > B600 > B > B800 > B1000. The pseudo-second-order model and Langmuir theoretical equation were used for fitting the kinetic and equilibrium data, respectively. Ion-exchange with Ca^{2+} and specific cation sorption were identified as main removal mechanisms. The amounts of Co^{2+} desorbed from loaded bone sorbents increased with the decrease of pH as well as with the increase of Ca^{2+} concentration. Heating at 400 °C was found to be an optimal treatment for the production of the Co^{2+} removal agent.

© 2008 Elsevier B.V. All rights reserved.

1. Introduction

Sorption is a simple and attractive method for heavy metal removal from aqueous effluents due to its high efficiency and easy handling. Economical feasibility of such processes can be gained by application of low-cost sorbents which are abundant in nature, or arise as a by-products or waste materials from various industries and require little processing [1].

Various biological materials were studied with the main aim to develop a cheap, reliable and more effective alternative to traditional treatment methods for metal-containing effluents. Most research has been carried out with microbial biomass, chiefly bacteria, algae and fungi [2]. More recently, waste materials from food and agricultural industry (wool, rice, straw, coconut husks, exhausted coffee, waste tea, orange peel, animal bones, eggshells, etc. [3]) are being considered as sorbents. Differently treated animal bones were also subjected to immobilization studies of metal cations such as Cu^{2+}, Cr^{3+}, Pb^{2+}, Zn^{2+}, Sr^{2+} [4–8], and radionuclides: ^{124}Sb^{3+}, ^{124}Sb^{5+}, ^{152}Eu^{3+} [9] as well as U(VI) [10].

Bones consist about 30% by weight of organic compounds, mainly fibrous protein collagen, while the remaining 70% represent inorganic phase composed of defect, poorly crystalline, cation and anion substituted hydroxyapatite Ca$_{10}$(PO$_4$)$_6$(OH)$_2$ (HAP) [11].

Generally, HAP was found to be a suitable sorbent for heavy metals and radioisotopes due to low water solubility, high stability under reducing and oxidizing conditions, high specific surface area and good buffering capacity [12]. The main cation removal mechanisms by HAP are ion-exchange reaction with calcium ions of the apatite, dissolution of HAP followed by the precipitation of metal-containing phosphate phases, and specific cation sorption on the HAP surface [12]. Animal bones, therefore, represent a source of biogenic apatite and a cost-effective alternative to synthetic HAP.

In contrast to other heavy metals and radionuclides, no data of Co^{2+} sorption by animal bones was found in literature. Cobalt containing effluents arise from the metallurgical industries while radioactive isotope, ^{60}Co, is a frequent constituent of liquid radioactive waste.

Considering good sorption properties of synthetic HAP powder towards Co^{2+} [13], the main aim of this study was to evaluate bone origin sorbents as Co^{2+} immobilization agents. Sorption efficiency of powdered bones, as well as of samples obtained by chemical oxidation and temperature treatments, was studied and compared at different pH, contact times and initial metal concentrations, while the stability of Co-loaded bone products was tested in the solutions of different pH and Ca^{2+} concentration. The correlation between treatments, physicochemical characteristics and sorption properties was established.

* Corresponding author. Tel.: +381 11 2453867.
E-mail address: sdimovic@vin.bg.ac.yu (S. Dimović).

2. Materials and methods

2.1. Preparation of bone sorbents

Bovine (femur) bones were collected from local butchers shop. The bones were cleaned from meat and cut by circular saw to peaces of approximate size 2–5 cm. Subsequently, bones were boiled in distilled water for 2 h, in order to remove fat this process was repeated three times. The bones were then transferred to the oven for drying at 80 °C. After 24 h, they were divided into six parts of about 300 g each. First part, denoted as B, was just milled and sieved, and the fraction of particles size 45–200 μm was used in further experiments. Second part, named BH$_2$O$_2$, was treated with an oxidation agent (30% H$_2$O$_2$) in order to remove the organic phase of the bone. The H$_2$O$_2$ solution was changed daily and heated up to the boiling temperature, three times a day. The process was stopped after 7 days, when no visible reaction occurred, and the sample was dried for 24 h, at 80 °C. The remaining four parts, denoted as B400–B1000, were annealed in an electric furnace under ambient condition, at four different temperatures (400, 600, 800 and 1000 °C), for 4 h. Sample BH$_2$O$_2$ as well as B400–B1000 were milled and sieved in order to collect the same particle size as for sample B.

2.2. Characterization of bone sorbents

Sample B was characterized by thermal decomposition measurement, using a SDT Q-600 instrument (TA Instruments). The sample (10.549 mg) was heated in a standard alumina 90 μl pan, in 100 ml/min flow of dynamic air in the temperature range 20–900 °C at a heating rate of 20 °C/min.

All prepared sorbents were analyzed by X-ray diffraction (XRD), using a Bruker D8 Advance diffraction system, with Cu K$\alpha_{1.2}$ radiation in theta/theta reflection geometry. The patterns were registered in the 2θ range from $8° < 2\theta < 60°$ with a scanning step size of 0.05° and an acquisition time of 4 s/step.

The specific surface area (S_p) of bone sorbents was determined applying 5-points BET method using nitrogen as an adsorbate, at 77 K. The measurements were performed with Autosorb-Quantochrome Model AS-6/P°. Samples were previously degassed under vacuum at 100 °C.

IR spectral examinations were performed by Bomem MB 100 FTIR spectrometer. The spectra were recorded in the 4000–500 cm^{-1} region, collecting 10 scans per spectrum, with a resolution of 4 cm^{-1}, using potassium bromide pellet technique. Pellets were prepared using 1 mg sample/15 mg KBr.

The batch equilibration technique, described in the literature in detail [14], was applied for the point of zero charge (pH$_{PZC}$) determination, using 0.1 M KNO$_3$ as a background electrolyte, in initial pH range 1–12.

2.3. Sorption/desorption experiments

Efficacy of bone sorbents for Co^{2+} immobilization was compared in a batch system. Solutions of different Co^{2+} concentrations were prepared from Co(NO$_3$)$_2$·6H$_2$O (Merck) and distilled water. PVC flasks, containing suspensions with solid to liquid ratio 1:200, were agitated in a horizontal shaker at constant speed of 120 rpm and ambient temperature (20 ± 1 °C).

Unless sorption parameter was the process variable, the following conditions were applied: initial Co^{2+} concentration 6×10^{-3} mmol/dm^3, initial pH 5, time of equilibration 24 h. The effect of sorption parameters was investigated by varying:

- initial pH in the range 1–12.

- contact time in the range 15 min to 48 h.
- initial Co^{2+} concentration in the range 10^{-4} to 6×10^{-3} mol/dm^3.

After separation of sorbents from the liquid phase by filtration through blue-band filter paper (Quant, Grade 391) the final solution pH values were measured. The exact initial and final concentrations of Co^{2+} were determined by an atomic absorption spectrometer (PerkinElmer Analyst 200), as well as concentrations of Ca^{2+} ions, released from the sorbents to the liquid phase.

For desorption studies, bone particles were firstly loaded with Co^{2+} ions by equilibrating the sorbents with the 6×10^{-3} mol/dm^3 Co^{2+} solution, at solid to liquid ratio 1:200, for 24 h. Solid residues were washed with distilled water in order to remove the unsorbed metal ions attached to the surface. The particles were then dried at 105 °C, transferred to PVC flasks and shaken with different leaching solutions, at solid to liquid ratio 1:200 for 24 h. After filtration, the metal concentration measurements in the supernatants were performed.

Leaching solutions of pH 2, 5, 7 and 9 were prepared using distilled water and appropriate amounts of 0.01 mol/dm^3 HNO$_3$ or KOH. Furthermore, 10^{-3}, 10^{-2} and 2.5×10^{-2} mol/dm^3 Ca(NO$_3$)$_2$ solutions were used.

3. Results and discussion

3.1. Physicochemical properties of bone sorbents

The TGA/DTA plot recorded from powdered B sample (Fig. 1) shows three distinctive successive weight losses with 56.33% inorganic residue available. Due to the release of absorbed water molecules a weight loss of 7.37% was recorded at temperature interval 20–200 °C, with the peak on the DTA plot positioned at 81 °C. In the second step, a mass reduction of 25.31% could be associated with the decomposition of collagen that started after 200 °C and continued up to 400 °C (DTA peak at 370.22 °C). In the temperature range 400–640 °C, with the peak at 471.87 °C, weight loss was 9.11% due to combustion of the residual organic components. Additionally 1.88% of weight loss was observed in temperature range 640–900 °C, and can be attributed to the decomposition of carbonates.

The XR-diffraction patterns of investigated samples (Fig. 2), confirmed that HAP was the main crystalline phase present, while a broad and intense background was associated with collagen and other organic compounds.
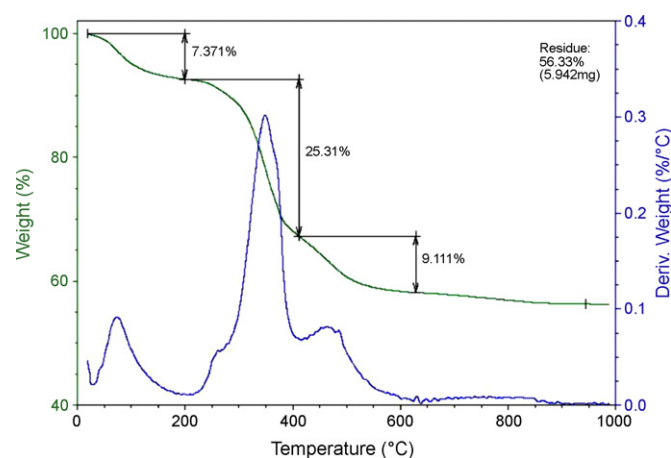

Fig. 1. DTA/TGA analysis of bone sample.

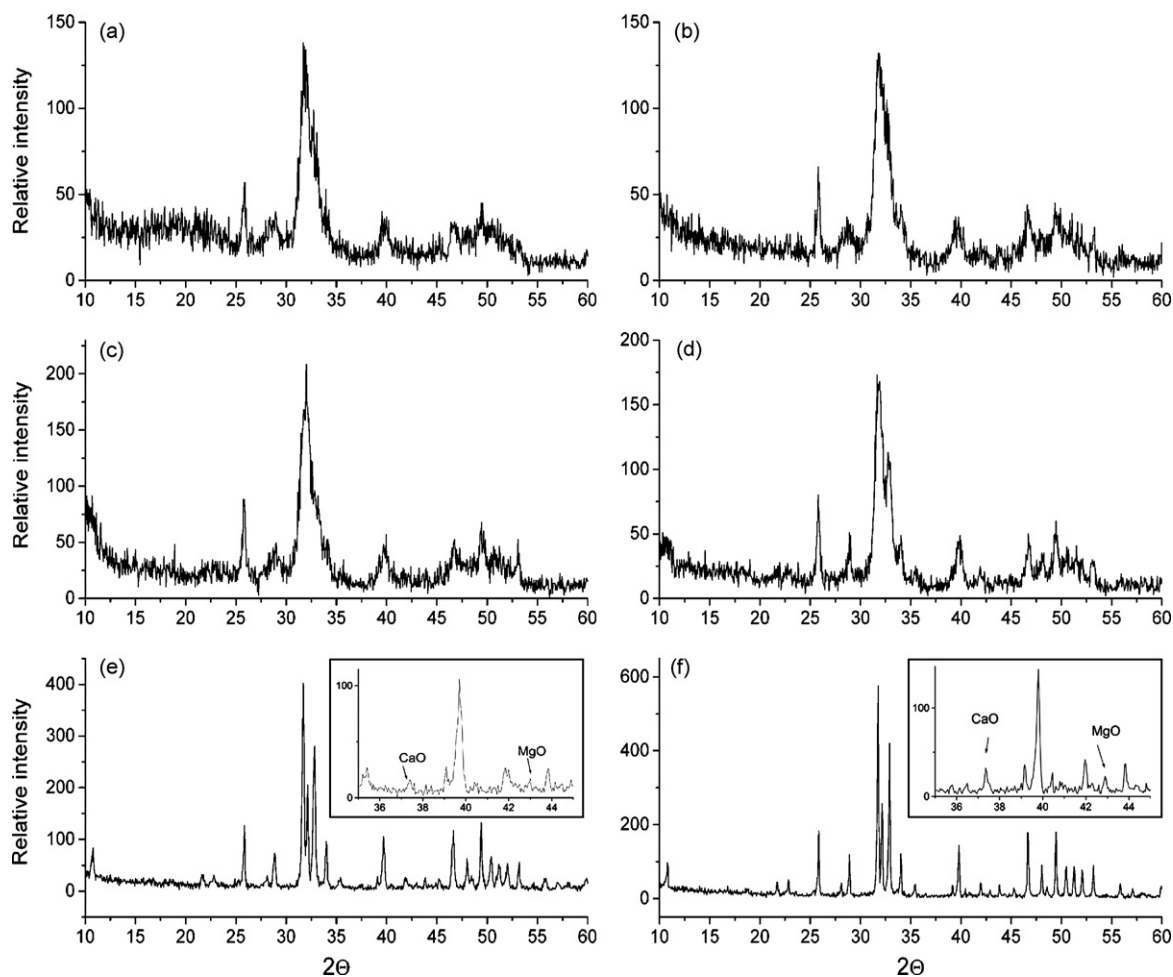**Fig. 2.** XRD patterns of bone sorbents: (a) B, (b) BH_2O_2, (c) B400, (d) B600, (e) B800 and (f) B1000.

The crystallinity grade (X_c) of the HAP powders can be evaluated by an experimental method reported by Landi et al. [15], using the equation:

$$X_c = 1 - \frac{V_{112/300}}{I_{300}} \tag{1}$$

where I_{300} is the intensity of (300) reflection and $V_{112/300}$ is the intensity of the hollow between (112) and (300) reflections, which completely disappears in non-crystalline samples. The X_c values of bone samples are summarized in Table 1.

Treatment with H_2O_2 as well as heating up to 400 °C did not create notable changes of HAP original crystallinity. In contrast, HAP crystallinity increased slowly from 400 to 600 °C, remarkably from 600 to 800 °C and remained almost constant from 800 to 1000 °C. The XRD patterns of the powders obtained at 800 and 1000 °C were similar to the patterns of the well-crystallized synthetic HAP [14].

Table 1
The fraction of crystalline phase, specific surface area and point of zero charge of bone samples

Sample	X_c	S_p (m²/g)	pH_{PZC}
B	0.26	0.1	7.22
BH_2O_2	0.27	83.0	6.83
B400	0.27	85.0	7.37
B600	0.36	71.7	7.50
B800	0.93	7.0	10.15
B1000	0.95	2.4	10.00

Additionally, in the spectra of these two samples, trace amounts of CaO and MgO were observed (Fig. 2e and f) and can be ascribed to the decomposition of non-stoichiometric carbonate containing bone apatite [16].

The characteristic bands of natural HAP were also detected in the IR spectra (Fig. 3).

The peaks at about 1090, 1040, 960, 601 and 570 cm⁻¹ arised from different vibrations of PO_4^{3-} group. In addition, the spectrum of sample B contained a band at 1160 cm⁻¹ that can be ascribed to HPO_4^{2-} group, while in the spectra of samples B600, B800 and B1000, in the region 1997–2200 cm⁻¹ overtones and combinations of the PO_4^{3-} modes were visible. The broad band from 3700 to 2500 cm⁻¹, the most intensive in the spectra of B and BH_2O_2 sample, derived from stretching modes of hydrogen-bonded H_2O molecules. Peaks at about 1410 and 1450 cm⁻¹, and near 870 and 670 cm⁻¹ could be attributed to the CO_3^{2-} group. The intensity of these peaks diminished with the temperature increase. The OH⁻ bands at 3572 and 629 cm⁻¹ were clearly visible only in the IR spectra of the heated samples B800 and B1000.

Additional peaks that came from the organic phase were also found. In the IR spectra of sample B, at 1547–1559, 1237 and 665–669 cm⁻¹ amide I, II and III bands, respectively, were visible. The peaks at 2923 and 2981 cm⁻¹ occurred due to vibrations of –CH₂ groups, while at 1744 cm⁻¹ carbonyl groups were detected. In the BH_2O_2 spectra, band at 1744 cm⁻¹ was completely removed, while other bands were present with the reduced
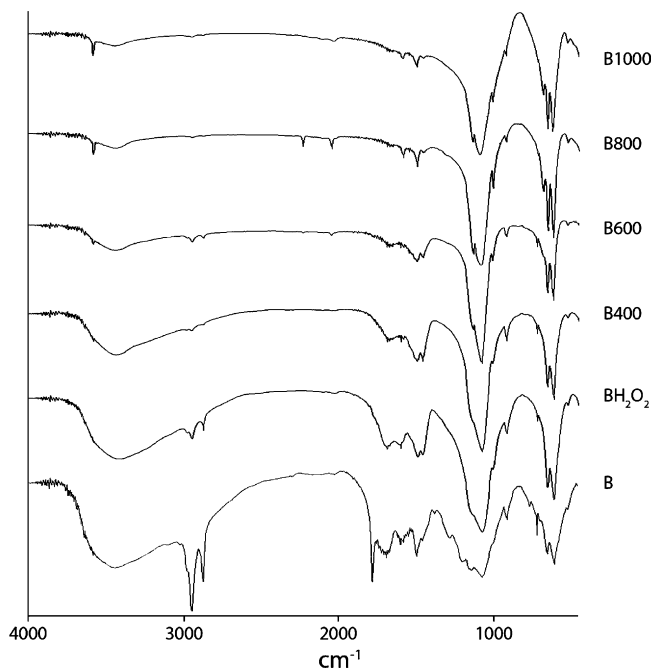
Fig. 3. FT-IR spectra of differently treated animal bones.

intensities. Heating of the bone sample was found to be more efficient approach in reducing the amount of organic phase, since in the samples B400 and B600 small –CH$_2$ and amide I bands were visible, while in B800 and B1000, only inorganic phase remained.

The S_p values of various bone sorbents are listed in Table 1. Although the mineral phase of bone consists of nano-sized crystals with high surface area (100–200 m^2/g) [17], merged with collagen fibers they give a structure of very high density, and consequently low surface area. Treatment with H$_2$O$_2$ and heating the bone sample to 400 °C have produced a significant S_p increase, which can be attributed to oxidation of bone organic compounds and their partial removal from the pores of the inorganic skeletal material. The decrease of S_p with the increase of temperature above 400 °C, can be explained by an increase of HAP crystallite size (Fig. 2 and Table 1).

The results of pH$_{PZC}$ determination are shown in Fig. 4.

The similar behavior of all investigated samples is obvious: final pH values increased as the initial pH has increased in the ranges 1–4 and 10–12, while maintained constant in the initial pH range 4–10. However, final pH values at the plateaus, from which points of zero charge (pH$_{PZC}$) were estimated (Table 1), differed significantly from 6.83 to 10.15. The pH$_{PZC}$ of all bone samples were higher with respect to the values obtained by the same method for various synthetic HAP samples [14]. Sample B, and those treated at 400 and 600 °C have demonstrated a small increase of pH$_{PZC}$ with the increase of temperature, while samples heated at 800–1000 °C had extremely high pH$_{PZC}$ values due to CaO and MgO occurrence (Fig. 2).

3.2. Effect of pH

The effect of initial pH on the sorption of Co^{2+} by bone origin sorbents is shown in Fig. 5a.

The predominant Co-species in the investigated pH range are Co^{2+} (pH < 8), and Co(OH)$_2$ (pH > 8). Experimental data suggested that removal of cobalt from the liquid phase occurred due to sorption of Co^{2+} species up to pH 8, whereas enhanced removal at pH > 8

(near 100%) regardless of the sorbent type, can be explained by precipitation of cobalt-hydroxide. Optimal sorption, for all considered sorbents, was obtained in the initial pH range 4–8. Relatively constant amounts of Co^{2+} sorbed in this initial pH range was a result of stable final pH values, governed by buffering capacity of the sorbents (Fig. 5b). The plateau parts of pH$_{final}$ versus pH$_{initial}$ plots were shorter when compared to the same experiment performed in inert electrolyte solution (Fig. 4), principally because of Co^{2+} hydrolysis. Furthermore, final pH values at the plateau parts of these plots were lower then the pH$_{PZC}$ values of each sorbent. The similar results were obtained for Co^{2+} sorption on synthetic HAP [13].

The amounts of Ca^{2+} released from inorganic phase of various bone sorbents showed comparable dependencies on initial pH (Fig. 5c). Ca^{2+} content decreased rapidly with the initial pH increase from 1 to 3, remained constant in the range 4–8 and decreased again at pH > 8. Enhanced HAP solubility in acidic media [18] caused high discharge of Ca^{2+} ions, while in the pH range of importance for sorption process (4–8) Ca^{2+} release was mainly due to ion exchange with Co^{2+} ions. As Co^{2+} removal occurred at pH below the pHpzc, where net surface charge of sorbent was positive, it can be concluded that specific cation sorption (e.g. ligand exchange) was also involved in the overall sorption mechanism [19].

Further sorption experiments were conducted at pH 5 in order to avoid dissolution of bone sorbents in acidic and Co^{2+} precipitation in alkaline solutions.

3.3. Effect of contact time

The removal of Co^{2+} ions by various bone sorbents as a function of contact time is presented in Fig. 6a. It was observed that the amounts of Co^{2+} sorbed increased with an increase in contact time and gradually reached constant values within 24 h.

The pseudo-first-order [20], pseudo-second-order [21] and intraparticle diffusion [22] models were tested to interpret the experimental data of investigated sorption processes. Based on the poor regression coefficient (R^2) values of the Lagergren pseudo-first-order, as well as intraparticle diffusion model, the results are not shown. The pseudo-second-order equation can be written in
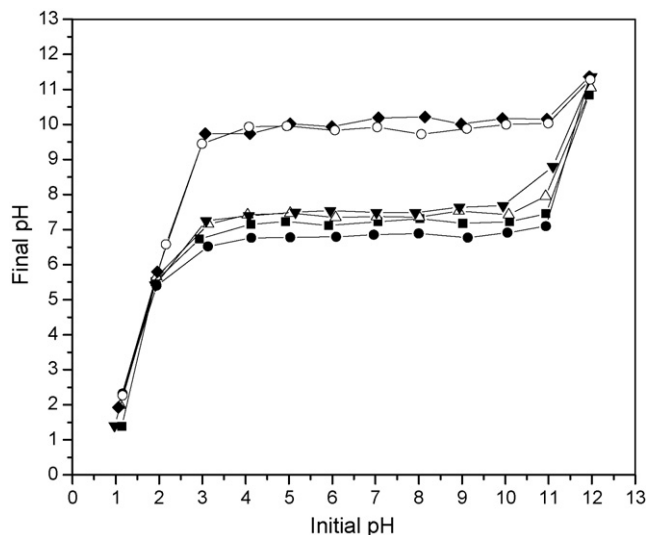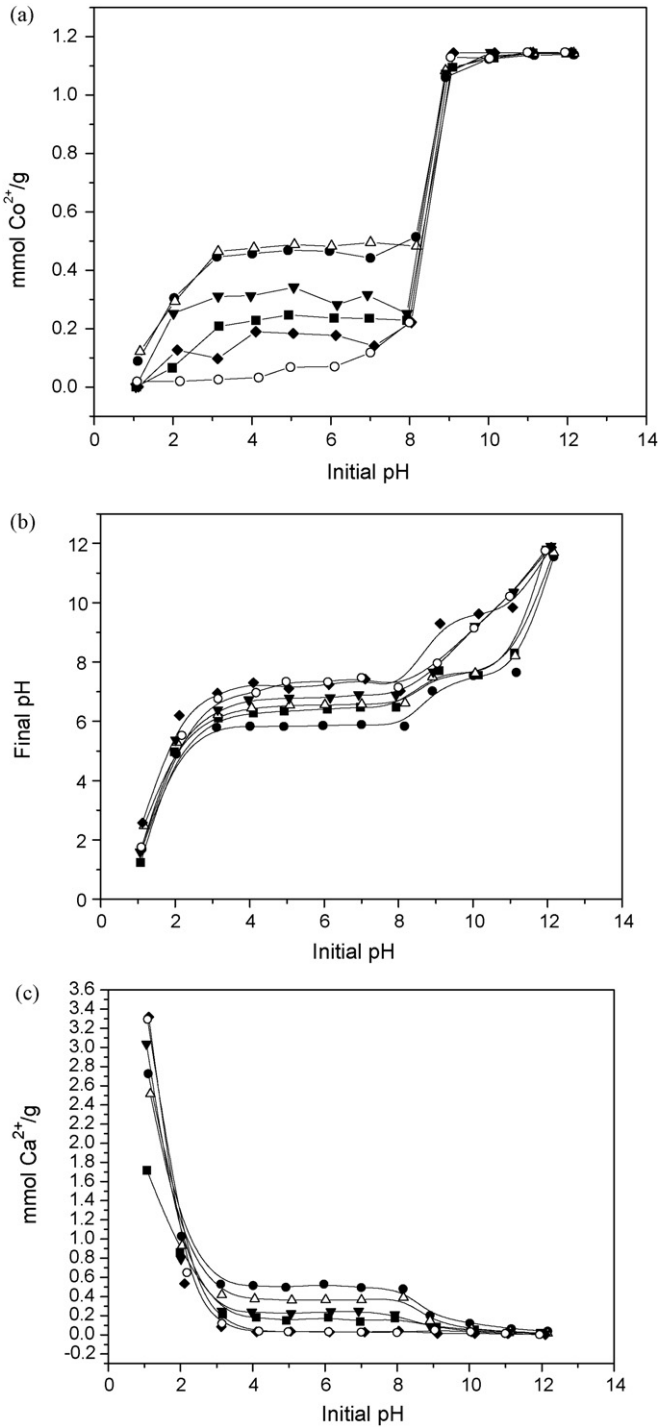

Fig. 4. The influence of the initial pH on the final pH values. Background electrolyte 0.1 mol/L KNO$_3$, sorbents: (■) B, (●) BH$_2$O$_2$, (△) B400, (▼) B600, (♦) B800 and (○) B1000.

when $t \rightarrow 0$, can also be calculated as follows:

$$h = k_2 q_e^2 \qquad (3)$$

Both high correlation coefficients ($R^2 > 0.993$) and good agreement between experimental and calculated q_e values indicated that the pseudo-second-order kinetic model can represent the sorption kinetics. Previous studies have also reported that the

Fig. 5. Effect of initial pH on the amounts of Co^{2+} sorbed (a), final pH values (b) and amounts of Ca^{2+} released (c). Sorbents: (■) B, (●) BH$_2$O$_2$, (△) B400, (▼) B600, (♦) B800 and (○) B1000.

the following linear form:
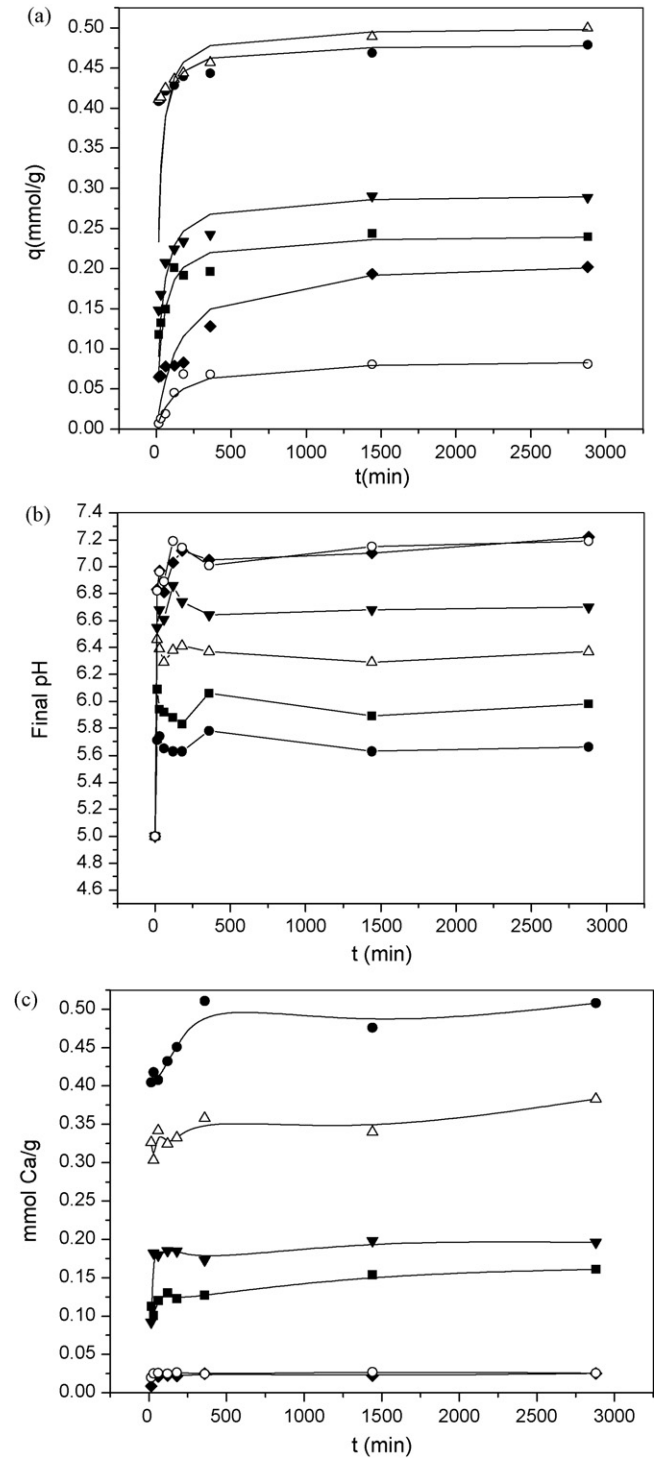
$$\frac{t}{q_t} = \frac{1}{k_2 q_e^2} + \frac{1}{q_e} t \qquad (2)$$

where k_2 (g/(mmol min)) is the pseudo-second-order rate constant, q_e the amount of Co^{2+} sorbed (mmol/g) at equilibrium and q_t is the amount sorbed (mmol/g) at any time t. From the slopes and intercepts of the of t/q_t versus t plots, k_2 and q_e values were calculated (Table 2). Furthermore, the initial sorption rates h (mmol/(g min)),

Fig. 6. Effect of contact time: (a) amounts of Co^{2+} sorbed, symbols—experimental data, solid line—pseudo-second-order model fitting, (b) final pH values, (c) amounts of Ca^{2+} released. Sorbents: (■) B, (●) BH$_2$O$_2$, (△) B400, (▼) B600, (♦) B800 and (○) B1000.

Table 2
Pseudo-second-order model parameters for Co^{2+} sorption by bone sorbents

Parameter	Sorbent					
	B	BH_2O_2	B400	B600	B800	B1000
$q_{e,exp.}$ (mmol/g)	0.240	0.478	0.499	0.290	0.202	0.080
q_e (mmol/g)	0.243	0.479	0.501	0.292	0.211	0.085
$h \times 10^2$ (mmol/(g min))	0.67	3.47	2.91	0.87	0.12	0.24
k_2 (g/(mmol min))	0.114	0.151	0.116	0.120	0.031	0.089
R^2	0.999	0.999	0.999	0.999	0.993	0.997

pseudo-second-order model correlates well with the experimental data on the sorption of divalent metal cation by synthetic HAP [23], Cr^{3+} by animal bones [7] and Sr^{2+} by bone char [8].

The highest initial sorption rates were obtained for samples BH_2O_2 and B400 which exhibited the highest surface area.

The plots of pH changes versus time (Fig. 6b), with a sharp increase in the first 30 min of contact, were very similar to results obtained for Cu^{2+} sorption onto bone char [24]. The buffering capacities of bone sorbents were responsible for pH_{final} increase. The order of equilibrium pH increase followed the order of pH_{PZC} increase: $BH_2O_2 > B > B400 > B600 > B800 > B1000$. However, as equilibrium pH values were lower than corresponding pH_{PZC}, the existence of specific cation sorption was confirmed.

The amounts of ion-exchanged Ca^{2+} cations (Fig. 6c) also increased with time, for all investigated sorbents, until equilibrium was reached.

Based on kinetic data, the equilibration time of 24 h was chosen for further study.

3.4. Effect of initial Co^{2+} concentration

The sorption isotherms of Co^{2+} on various bone samples are presented in Fig. 7a. Experimentally obtained sorption capacities were in the range 0.077–0.490 mmol/g, while affinity of the investigated sorbents towards Co^{2+} decreased in the following order: $B400 > BH_2O_2 > B600 > B > B800 > B1000$.

The experimental results were fitted with the Langmuir theoretical model, which has provided a reliable description of many systems in which metal cations in solution undergo surface sorption or ion-exchange [25]. It can be expressed in a following linear form:

$$\frac{C_e}{Q_e} = \frac{1}{X_m K_L} + \frac{C_e}{X_m} \tag{4}$$
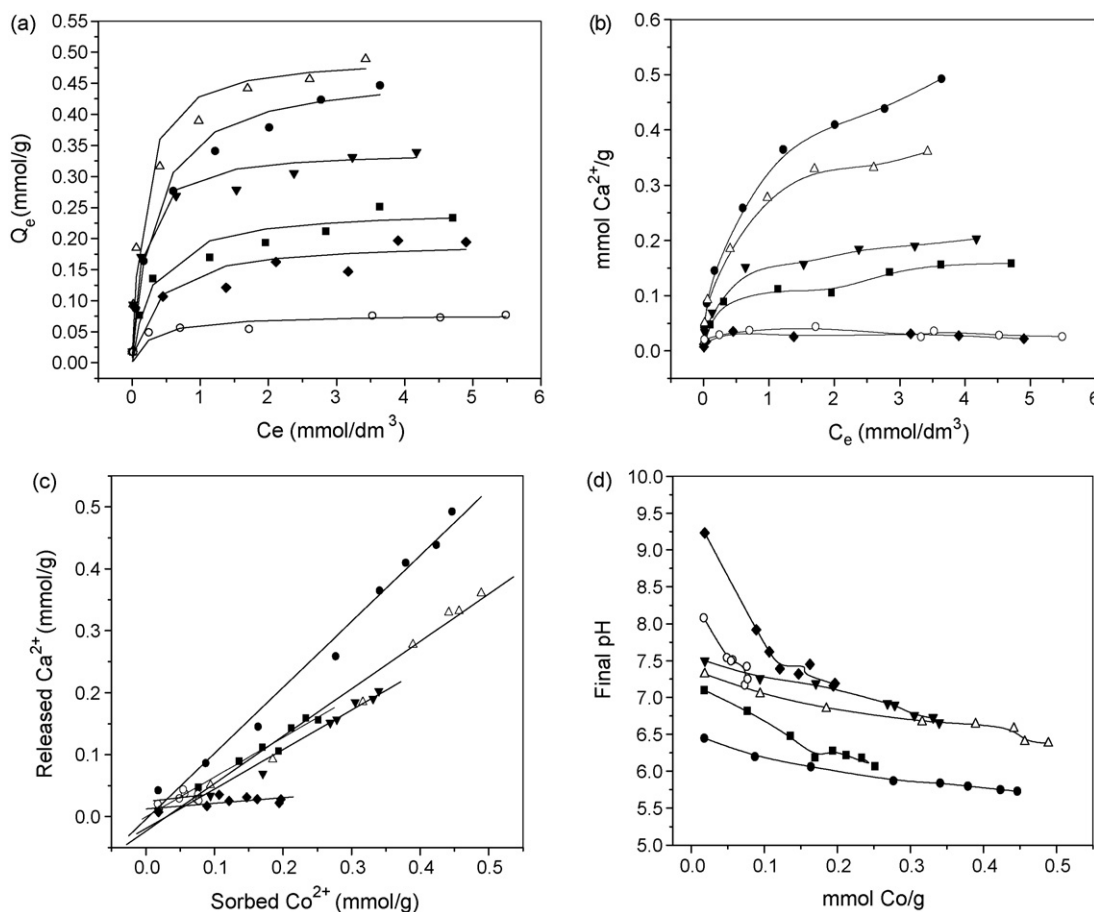
Fig. 7. (a) Relationships between equilibrium Co^{2+} concentrations and the amounts of Co^{2+} sorbed, symbols—experimental data, solid line—Langmuir fitting, (b) relationships between equilibrium Co^{2+} concentrations and the amounts of Ca^{2+} released, (c) molar ratios between sorbed and released metal cations and (d) functionalities between the amounts of Co^{2+} sorbed and final pH values. Sorbents: (■) B, (●) BH_2O_2, (△) B400, (▼) B600, (◆) B800 and (○) B1000.

Table 3
The results of equilibrium data fitting using Langmuir equation

Sorbent	X_m (mmol/g)	K_L (dm^3/mmol)	R^2	$X_{m,exp}$ (mmol/g)
B	0.248	3.343	0.985	0.234
BH$_2$O$_2$	0.469	3.128	0.992	0.447
B400	0.495	6.608	0.996	0.490
B600	0.342	6.868	0.995	0.340
B800	0.195	2.893	0.954	0.197
B1000	0.078	3.602	0.984	0.077

Table 4
Maximum Co^{2+} sorption capacities for a range of low-cost sorbents

Sorbent	Sorption capacity (mmol/g)	Ref.
Anaerobic granular sludge	0.209	[26]
Coir pith	0.218	[27]
Arca shell	0.132	[28]
Seaweeds	0.350	[29]
Activated carbon	0.236	[30]
Tobermorite	0.178	[31]
Natural zeolites	0.244	[32]
Kaolinite	0.016	[33]
Hydrated manganese dioxide	0.210–0.682	[34]
Synthetic	0.300	[35]
HAP	0.343	[13]
Treated animal bones	0.078–0.495	This study

where Q_e (mmol/g) and C_e (mmol/dm^3) denotes the equilibrium concentrations of sorbate in the solid and the liquid phase, X_m (mmol/g) is the maximum sorption capacity, and K_L (dm^3/g) is the Langmuir constant related to the energy of adsorption.

The results of linear fitting are presented in Table 3. High correlation coefficients were obtained for all investigated systems ($R^2 > 0.954$), and the calculated capacities corresponded with the experimentally obtained values.

The maximum Co^{2+} removal capacities of differently treated animal bones, B400 and BH$_2$O$_2$ in particular, were comparable or better than the capacities of many other sorbent materials, reported for single metal batch conditions (Table 4).

The amounts of Ca^{2+} cations released per gram of each bone sorbent at equilibrium increased with the increase of the amounts of Co^{2+} sorbed (Fig. 7b). The molar ratios between Ca^{2+} released and Co^{2+} sorbed, were relatively constant, making functionalities between released and sorbed cations linear (Fig. 7c). However, slopes of those lines fluctuated significantly between sorbents—decreased in the order BH$_2$O$_2$ (1.06) > B400 (0.76) > B (0.64) > B600 (0.63) > B1000 (0.12) > B800 (0.09), which indicated that the participation of ion-exchange mechanism decreased in the same way.

With the increase of the amount of cation sorbed a continuous final pH decrease was observed, regardless of the sorbent type (Fig. 7d). It also must be noted that using B800 and B1000 samples and solution of the lowest Co^{2+} concentration, values

of pH$_{final}$ > 8 were obtained meaning that Co(OH)$_2$ precipitation might have occurred. The comparison of specific cation sorption contribution, calculated as a difference between pH$_{PZC}$ and pH$_{final}$ values at the maximum amount of Co^{2+} sorbed, increased in the following order B600 (0.84) > B400 (0.99) > B (1.04) > BH$_2$O$_2$ (1.10) > B1000 (2.75) > B800 (2.99). Therefore, the contribution of specific cation sorption increased in the same order.

As the stability of HAP phase increase with the increase of solution pH [26], final pH values >7 obtained for B and B400–1000 samples may be the main reason for lower Ca^{2+} release and molar ratios Ca/Co < 1. This is particularly obvious for B800 and B1000 samples, which, on the other hand, exhibited the highest participation of specific cation sorption.

3.5. Correlation between treatments, physicochemical properties of bone samples and Co^{2+} sorption capacities

Comparing the results from Tables 1 and 3, the correlation between physicochemical properties of bone samples and Co^{2+} sorption capacities can be established. The amounts of Co^{2+} sorbed
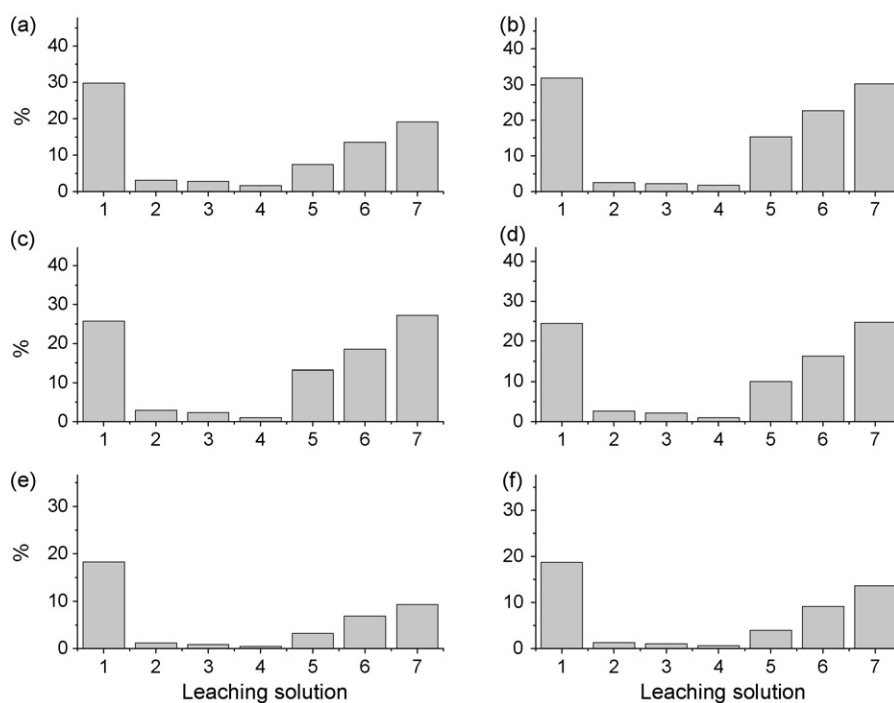
Fig. 8. Relative percentages of Co^{2+} ions desorbed from sample B (a), BH$_2$O$_2$ (b), B400 (c), B600 (d), B800 (e) and B1000 (f). Leaching solutions: (1) pH 2, (2) pH 5, (3) pH 7, (4) pH 9, (5) 0.001 mol/dm^3 Ca(NO$_3$)$_2$, (6) 0.01 mol/dm^3 Ca(NO$_3$)$_2$ and (7) 0.25 mol/dm^3 Ca(NO$_3$)$_2$.

Table 5
Leaching solutions initial pH values and final pH values obtained after desorption of Co^{2+} ions

Composition	Initial pH	Final pH					
		B	BH_2O_2	B400	B600	B800	B1000
Distilled water	2.00	5.19	5.14	5.34	5.47	5.82	5.71
Distilled water	5.00	6.61	6.46	6.72	6.78	6.93	6.75
Distilled water	7.00	6.79	6.50	6.85	6.89	7.04	6.86
Distilled water	9.00	6.88	6.85	6.96	6.98	7.18	6.98
Ca 0.001 mol/dm³	5.55	6.39	6.31	6.44	6.53	6.79	6.68
Ca 0.01 mol/dm³	5.49	6.27	6.18	6.38	6.49	6.66	6.61
Ca 0.25 mol/dm³	5.36	6.19	6.14	6.28	6.41	6.59	6.48

increased with the increase of S_p values, with an exception of sample B which exhibited lowest specific surface area and moderate sorption. This may be explained by the fact that organic phase of sample B, unlike in other treated samples, had high amounts of polar and negatively charged functional groups (Fig. 3) which were acting as binding sites for Co^{2+} ions.

Furthermore, the extent of sorption decreased with the increase of apatite crystallinity in the range 0.26–0.95. The specimens with the similar X_c values (B, B400 and BH_2O_2) differed in the sorbed amount of Co^{2+}, pointing out the role of bone organic phase: lower content of organic matter correlates with the higher sorption capacity.

The relationship between sorption capacities and pH_{PZC} values of bone sorbents was generally poor. Low sorption capacities of powders with extremely high pH_{PZC} values (B800 and B1000) were more likely related to other characteristics, such as low S_p and high X_c.

Previously reported results of the influence of synthetic HAP physicochemical properties (such as Ca/P ratio, solubility, pH_{PZC}, S_p, X_c, fluoride and carbonate substitutions, etc. [14,36,37]) onto sorption of divalent cations, have revealed that specific surface area is the most important factor determining sorption capacities. Our study supports these results. The optimal treatment for the production of Co^{2+} immobilization agent was found to be heating at 400 °C, since this sample exhibited the highest S_p value. The S_p of H_2O_2 treated sorbent was somewhat lower when compared to B400, nevertheless, this treatment was also efficient in organic phase dissociation and oxidation and the production of high capacity Co^{2+} sorbent.

3.6. Desorption study

The desorption efficiency of Co-loaded bone sorbents, tested using various leaching solutions, is presented in Fig. 8. It is obvious that Co^{2+} desorption was highly pH and Ca^{2+} concentration-dependent, exhibited the same trend for all sorbents: increase with the pH decrease and Ca^{2+} concentration increase.

Desorption of Co^{2+} was the most pronounced in solution of pH 2 (18–32%). Conversely, in alkaline media (pH 9) only about 1–3% of Co^{2+} was removed from bone sorbents. Under various pH conditions the most stable were B800 and B1000 Co-loaded products. The buffering properties of bone samples were responsible for increasing pH of acidic leaching solutions and decreasing pH of alkaline solution (Table 5).

Desorption in Ca^{2+} solutions showed the highest percentages in the case of BH_2O_2 sample and the lowest for B800 and B1000, following the same pattern as the contribution of ion-exchange in the overall sorption mechanism of investigated sorbents (Section 3.4).

Results from the present desorption study revealed that high amounts of previously sorbed Co^{2+} cations stayed attached to the bone sorbents surfaces, under all investigated experimental conditions, meaning that spent animal bones will require disposal rather than regeneration.

4. Conclusion

This investigation has demonstrated that animal bones, a waste product from meat industry, represent a suitable precursor material for the production of high capacity Co^{2+} sorbents. Bones were treated with an oxidation agent or annealed at different temperatures in order to evaluate the optimal treatment conditions. Physicochemical characterization of obtained products revealed that heating at 400 °C and chemical oxidation process caused partial removal of bone organic components with preservation of the poor apatite phase crystallinity, while heating at higher temperatures, especially $T > 600$ °C, caused sintering of HAP nanocrystals and decrease of specific surface area.

Co^{2+} removal efficiency by various bone sorbents was compared at different experimental conditions. Optimal sorption was obtained in the wide initial pH range 4–8, due to the excellent buffering properties of investigated materials. The kinetic data were well fitted with pseudo-second-order kinetic model and have revealed that, under applied experimental conditions, approximately 24 h was needed for attaining sorption equilibrium. The Langmuir isotherm described all equilibrium data adequately. The calculated maximum sorption capacities, which decreased in the order: B400 (0.495 mmol/g) > BH_2O_2 (0.469 mmol/g) > B600 (0.342 mmol/g) > B (0.248 mmol/g) > B800 (0.195 mmol/g) > B1000 (0.078 mmol/g), indicated that treated animal bones, particularly B400 and BH_2O_2, have comparable or better sorption capacities than various low-cost sorbents and synthetic HAP. Since the Co^{2+} sorption capacities were positively correlated with the lower crystallinity of the inorganic apatite phase and higher specific surface area, the optimal treatment for the production of Co^{2+} immobilization agent was found to be heating of animal bones at 400 °C.

The leaching studies demonstrated the great stability of Co-bone products. Desorbed amounts of Co^{2+} increased with pH decrease as well as with the increase of competitive cation (Ca^{2+}) concentration, while the highest amounts of Co^{2+} leached from various bone powders (18–32%) were obtained under acidic conditions (pH 2).

References

[1] S. Bailey, T.R. Olin, M.A. Dean, A review of potentially low-cost sorbents for heavy metals, Water Res. 33 (1999) 2469–2479.
[2] J. Wase, C. Forster (Eds.), Biosorbents for Metal Ions, Taylor & Francis, London, 1997.
[3] K. Chojnacka, Biosorption of Cr(III) ions by eggshells, J. Hazard. Mater. 121 (2005) 167–173.
[4] F. Banat, S. Al-Asheh, F. Mohai, Batch zinc removal from aqueous solution using dried animal bones, Sep. Purif. Technol. 21 (2000) 155–164.
[5] J.A. Wilson, I.D. Pulford, S. Thomas, Sorption of Cu and Zn by bone charcoal, Environ. Geochem. Health 25 (2003) 51–56.
[6] E. Deydier, R. Guilet, P. Sharrock, Beneficial use of meat and bone meal combustion residue: "an efficient low cost material to remove lead from aqueous effluent", J. Hazard. Mater. B101 (2003) 55–64.
[7] K. Chojnacka, Equilibrium and kinetic modelling of chromium(III) sorption by animal bones, Chemosphere 59 (2005) 315–320.
[8] I. Smičiklas, S. Dimović, M. Sljivić, I. Plećaš, The batch study of Sr^{2+} sorption by bone char, J. Environ. Sci. Health A 48 (2008) 210–217.
[9] M.W. Abdel Raouf, A.A.M. Daifullah, Potential use of bone charcoal in the removal of antimony and europium radioisotopes from radioactive wastes, Adsorpt. Sci. Technol. 15 (1997) 559–569.

[10] C.C. Fuller, J.R. Bargar, J.A. Davis, Molecular-scale characterization of uranium sorption by bone apatite materials for a permeable reactive barrier demonstration, Environ. Sci. Technol. 37 (2003) 4642–4649.

[11] T.S.B. Narasaraju, D.E. Phebe, Some physico-chemical aspects of hydroxylapatite, J. Mater. Sci. 31 (1996) 1–21.

[12] F. Monteil-Rivera, M. Fedoroff, Sorption of inorganic species on apatites from aqueous solutions. In: Encyclopedia of Surface and Colloid Science, Marcel Dekker, Inc., New York, 2002, pp. 1–26.

[13] I. Smičiklas, S. Dimović, I. Plećaš, M. Mitrić, Removal of Co²⁺ from aqueous solutions by hydroxyapatite, Water. Res. 40 (2006) 2267–2274.

[14] I. Smičiklas, A. Onjia, S. Raičević, Experimental design approach in the synthesis of hydroxyaptite by neutralization method, Sep. Purif. Technol. 44 (2005) 97–102.

[15] E. Landi, A. Tampieri, G. Celotti, S. Sprio, Densification behavior and mechanisms of synthetic hydroxyapatites, J. Eur. Ceram. Soc. 20 (2000) 2377–2387.

[16] K.D. Rogers, P. Daniels, An X-ray diffraction study of the effects of heat treatment on bone mineral microstructure, Biomaterials 23 (2002) 2577–2585.

[17] A.S. Posner, The structure of bone apatite surfaces, J. Biomed. Mater. Res. 19 (1985) 241–250.

[18] G.J. Levinskas, W.F. Neuman, The solubility of bone mineral. I. Solubility studies of synthetic hydroxyapatite, J. Phys. Chem. 59 (1959) 164–168.

[19] J. Hu, I.M.C. Lo, G. Chen, Comparative study of various magnetic nanoparticles for Cr(VI) removal, Sep. Purif. Technol. 56 (2007) 249–256.

[20] S. Lagergren, Zur theorie der sogenannten adsorption geloster stoffe, Kungliga Svenska Vetenskapsakademiens, Handlingar 24 (1898) 1–39.

[21] Y.S. Ho, G. McKay, Pseudo-second order model for sorption processes, Process Biochem. 34 (1999) 451–465.

[22] W.J. Weber, J.C. Morris, Kinetics of adsorption of carbon from solutions, J. Sanit. Eng. Div. Am. Soc. Civ. Eng. 89 (1963) 31–63.

[23] I. Smičiklas, A. Onjia, S. Raičević, Đ. Janaćković, M. Mitrić, Factors influencing the removal of divalent cations by hydroxyapatite, J. Hazard. Mater. 152 (2008) 876–884.

[24] C.W. Cheung, J.F. Porter, G. McKay, Sorption kinetics for the removal of copper and zinc from effluents using bone char, Sep. Purif. Technol. 19 (2000) 55–64.

[25] N.J. Coleman, Interactions of Cd(II) with waste-derived 11 Å tobermorites, Sep. Purif. Technol. 48 (2006) 62–70.

[26] E.D. van Hullebusch, A. Peerbolte, M.H. Zandvoort, P.N.L. Lens, Sorption of cobalt and nickel on anaerobic granular sludges: isotherms and sequential extraction, Chemosphere 58 (2005) 493–505.

[27] H. Parab, S. Joshi, N. Shenoy, A. Lali, U.S. Sarma, M. Sudersanan, Esterified coir pith as an adsorbent for the removal of Co(II) from aqueous solution, Bioresour. Technol. 99 (2008) 2083–2086.

[28] S. Dahiya, R.M. Tripathi, A.G. Hegde, Biosorption of heavy metals and radionuclide from aqueous solutions by pre-treated arca shell biomass, J. Hazard. Mater. 150 (2008) 376–386.

[29] K. Vijayaraghavana, J. Jegan, K. Palanivelu, M. Velan, Biosorption of cobalt(II) and nickel(II) by seaweeds: batch and column studies, Sep. Purif. Technol. 44 (2005) 53–59.

[30] E. Demirba, Adsorption of cobalt(II) ions from aqueous solution onto activated carbon prepared from hazelnut shells, Adsorpt. Sci. Technol. 21 (2003) 951–963.

[31] N.J. Coleman, D.S. Brassington, A. Raza, A.P. Mendham, Sorption of Co²⁺ and Sr²⁺ by waste-derived 11 tobermorite, Waste Manage. 26 (2006) 260–267.

[32] E. Erdem, N. Karapinar, R. Donat, The removal of heavy metal cations by natural zeolites, J. Colloid Interface Sci. 280 (2004) 309–314.

[33] Ö. Yavuz, Y. Altunkaynak, F. Güzel, Removal of copper, nickel, cobalt and manganese from aqueous solution by kaolinite, Water Res. 37 (2003) 948–952.

[34] A. Motl, F. Šebesta, J. John, I. Kadlecová, Sorption of cobalt on hydrated manganese dioxide, Czech. J. Phys. 49 (1999) 665–671.

[35] T. Suzuki, T. Hatsushika, M. Miyake, Synthetic hydroxyapatites as inorganic cation exchangers. Part 2, J. Chem. Soc., Faraday Trans. 78 (1982) 3605–3611.

[36] M. Peld, K. Tonsuaadu, V. Bender, M. Veiderma, Effect of fluoride and carbonate substitutions on apatites Cd²⁺ sorption capacity, Toxicol. Environ. Chem. 81 (2001) 43–53.

[37] N.C.C. Da Rocha, R.C. De Campos, A.M. Rossi, E.L. Moriera, A.D. Barbosa, G.T. Moure, Cadmium uptake by hydroxyapatite synthesized in different conditions and submitted to thermal treatment, Environ. Sci. Technol. 336 (2002) 1630–1635.